Astron. Astrophys. 327, 1194–1205 (1997)

ASTRONOMY AND ASTROPHYSICS

On the distance to the Chamaeleon I and II associations

D.C.B. Whittet[1,2], T. Prusti[3], G.A.P. Franco[4], P.A. Gerakines[1,5], D. Kilkenny[6], K.A. Larson[1], and P.R. Wesselius[2]

[1] Department of Physics, Applied Physics & Astronomy, Rensselaer Polytechnic Institute, Troy, NY 12180-3590, USA
[2] SRON, P.O. Box 800, 9700 AV Groningen, The Netherlands
[3] ISO Science Operations Centre, Astrophysics Division, ESA, Villafranca del Castillo, P.O. Box 50727, E-28080 Madrid, Spain
[4] Departamento de Física – ICEx – UFMG, Caixa Postal 702, 30.161-970 – Belo Horizonte – MG, Brasil
[5] Leiden Observatory, P.O. Box 9513, 2300 RA Leiden, The Netherlands
[6] SAAO, P.O. Box 9, Observatory, Cape 7935, South Africa

Received 23 December 1996 / Accepted 25 June 1997

Abstract. Constraints on the distances to the dark clouds Chamaeleon I and II are investigated in detail. A compilation of photometric data, spectral types and absolute magnitudes for field stars towards each cloud is presented, and results are used to examine the distribution of reddening with distance along each line of sight. The distances to stars associated with reflection nebulae in each cloud are examined in detail. On the basis of these results, we deduce the most probable distance of Cha I to be 160 ± 15 pc, and that of Cha II to be 178 ± 18 pc. An examination of the mean fluxes of T Tauri stars in each cloud provides independent evidence to suggest that Cha II is significantly more distant than Cha I. Both clouds appear to be embedded in a macroscopic sheet-like structure extending over much of the Chamaeleon-Musca-Crux region. The Chamaeleon III and DC 300.2–16.9 clouds are probably part of the same structure, with probable distances ∼140–160 pc.

Key words: stars: distances – ISM: clouds; dust, extinction; Chamaeleon clouds; reflection nebulae

1. Introduction

A knowledge of the distances to interstellar clouds associated with current or recent star formation is vitally important if the luminosities of newly formed stars are to be reliably determined. Other factors such as cloud mass estimates and space velocities of member stars are also distance-dependent. Unfortunately, distances are often difficult to determine with reasonable accuracy. Two principal methods have been applied. One is to determine spectrophotometrically the distances to selected individual stars which are known to be at the same distance as the cloud, due, for example, to the presence of reflection nebulosity. The second method is to investigate the dependence of reddening on distances for a large sample of field stars distributed along the line of sight: this allows a statistical determination of the distance at which there is a significant increase in reddening associated with dust in the cloud. The latter approach can work well for isolated clouds at intermediate Galactic latitude, such as those in Chamaeleon, where field stars can be found in sufficient numbers and the situation is uncomplicated by the presence of significant foreground extinction. The main sources of error associated with both methods are (i) uncertainties in stellar absolute magnitudes, and (ii) the possibility of a non-standard extinction law, typically involving increases in the ratio of total to selective extinction ($R_V = A_V/E_{B-V}$) as a function of the density of the dark-cloud material in the line of sight.

Chamaeleon contains three distinct dark clouds (Schwartz 1977; 1991), Cha I (DC 297.2–15.6), Cha II (DC 303.0–14.3) and Cha III (DC 303.0–17.1), together with a number of smaller structures, including a compact globule (the 'Thumbprint Nebula', FitzGerald 1974), and the isolated cloud DC 300.2–16.9 (Laureijs et al. 1989). To aid our discussion of the spatial distribution of these clouds, we present in Fig. 1 maps of 100 μm flux detected by the Infrared Astronomical Satellite (IRAS). Fig. 1a is a grey-scale flux plot of the area of sky containing the clouds, and Fig. 1b is a labelled contour map of the same region. The distances to all of these clouds are controversial. Estimates for Cha I range from 115 to 215 pc (Schwartz 1991), whilst star-count data suggest that the Thumbprint Nebula may be as far away as 400 pc (FitzGerald et al. 1976). The distance to Cha II is poorly constrained in previous literature. It is assumed to be bound by the distances to Cha I and the Thumbprint Nebula (Graham & Hartigan 1988), i.e. $115 \leq d(\text{Cha II}) \leq 400$ pc. The study of Franco (1991) supports a value (158 pc) at the lower end of this range, whereas Hughes & Hartigan (1992) favour a value of 200 pc. The distances to the other primary condensations in Fig. 1, Cha III and DC 300.2–16.9, are unknown. However, there is morphological and photometric evidence to suggest that all of these clouds may, in fact, be part of the same macroscopic structure (King et al. 1979; Franco 1991; Corradi

Send offprint requests to: D.C.B. Whittet

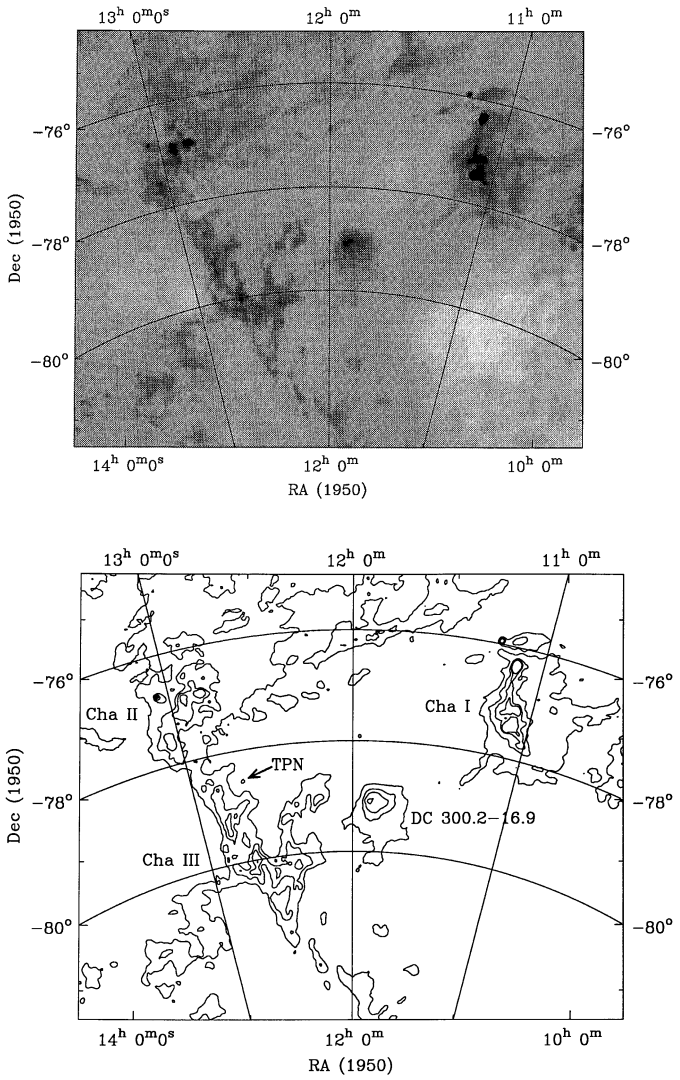

Fig. 1a and b. IRAS maps of the Chamaeleon region in 100 μm flux: **a** grey-scale flux plot, and **b** labelled contour map. The maps have identical position, scale and orientation.

et al. 1997), as suggested by Fig. 1, where linking bridges and striations can be seen (Cha II and Cha III, in particular, seem likely to be physically associated). Their distances may thus be closely similar, or geometrically related in a simple way.

Evidence for extensive current or recent star formation has been found in both Cha I and Cha II (e.g. Prusti et al. 1992a, b; Gauvin & Strom 1992; Hartigan 1993; Chen et al. 1997; see Schwartz 1991 for a summary of earlier work). The Cha I cloud contains a prominent T-association. A compilation of data for young member stars, and the resulting luminosity function, can be found in Prusti et al. (1992a). Star formation in Cha II is currently under intensive investigation. Much attention has been focused on the Herbig-Haro objects HH 52–54, their source of excitation, and associated molecular flows (Graham & Hartigan 1988; Hughes et al. 1991; Knee 1992; Nisini et al. 1996). The spectral energy distributions of optically identified pre-main-sequence stars throughout Cha II have been studied by Whittet et al. (1991a), whilst Prusti et al. (1992b) have used the IRAS database to identify further candidate young stellar objects in the region. The luminosity function for Cha II is determined by Larson et al. (1997). Isolated cases of star formation have also been identified in DC 300.2–16.9 (Alcalá et al. 1993) and in the vicinity of HD 104237, which lies between Cha I and Cha II (Knee & Prusti 1996). Uncertainties in the distance to the clouds have impact on all of these investigations.

2. The distance to Chamaeleon I

2.1. The distribution of reddening

Whittet et al. (1987) estimated the distance to Cha I by investigating the distribution of reddening suffered by field stars seen in projection against the cloud. Since the time of this study, additional broadband visual and near infrared photometry has been published for a number of stars in the field star catalogue, allowing precise evaluation of reddening and extinction parameters for a considerably larger number of stars than was previously possible (see Whittet et al. 1994 and references therein). A reassessment is therefore timely. Table 1 presents a compilation of relevant data (visual magnitudes, MK spectral types, E_{B-V} color excesses and R_V values; see Whittet et al. 1994 for original references). Two objects in the original field star catalogue, F29 and F34, are omitted as they were shown to be members of the T-association by Whittet et al. (1994, appendix). Absolute magnitudes ($M_V^{\rm sp}$) based on MK spectral types, using the calibration of Schmidt-Kaler (1982), are given for all stars in Table 1. Calculated distances (d) are listed in the final column.

To further refine reddening and distance estimates for selected field stars, we made observations in the Strömgren $uvby\beta$ photometric system with the Modular Photometer on the 0.5 m telescope at the South African Astronomical Observatory (SAAO) in 1997 February. Resulting Strömgren parameters for 14 stars are listed in Table 2. Strömgren photometry for a few additional Cha I stars is available from the work of Corradi & Franco (1995). For consistency with broadband data, all reddening values in the Strömgren system are converted to the Johnson system (see Table 1) via the standard relation $E_{B-V} = E_{b-y}/0.74$ (Crawford 1975a). The β-index provides an independent (photometric) estimate of absolute magnitude ($M_V^{\rm ph}$) for these stars (Crawford 1975b, 1978, 1979). The agreement between photometric and spectroscopic absolute magnitudes is generally reasonable (the standard deviation of the difference, $M_V^{\rm sp} - M_V^{\rm ph}$, is comparable with the error of measurement). We adopt the average of $M_V^{\rm sp}$ and $M_V^{\rm ph}$ for determination of the distances to these stars.

The reddening vs. distance relation based on Table 1 is shown in Fig. 2. Stars with Strömgren photometry available are distinguished by plotting symbol from those with absolute magnitudes based only on MK types; the latter are further distinguished according to luminosity class, as main sequence stars generally have smaller errors in M_V^{sp} than giants or subgiants (see Schmidt-Kaler 1982). The locus of the embedded zero-age

Table 1. Catalogue of reddenings, distances and related information for field stars in the line of sight to Chamaeleon I. The 'F' notation is from Whittet et al. (1987). Spectral classifications and photometric data are from the compilation of Whittet et al. (1994) unless otherwise indicated in the notes (see Table 6 of that paper for references). Absolute magnitudes $M_V^{\rm sp}$ and $M_V^{\rm ph}$ are deduced from MK spectral types and *uvbyβ* photometry, respectively; when both are available, a mean is used to calculate distance. R_V = 3.1 is assumed when no other value is given.

Star	V	Sp	$M_V^{\rm sp}$	$M_V^{\rm ph}$	E_{B-V}	R_V	d (pc)	Notes
Cha I F1	10.31	K4 III	0.0	—	0.14	—	944	
Cha I F2 = CPD−77°646	9.90	B8 V	−0.25	—	0.58	3.3	444	
Cha I F3 = HD 94414	7.99	B4 V	−1.4	−0.7	0.65	3.1	254	1, 2
Cha I F4 = HD 94454	6.67	B8 III	−1.2	—	0.23	3.1	270	
Cha I F5 = HD 94716	9.00	B9 V	0.2	—	0.22	—	420	
Cha I F6	11.06	A2 V	1.3	—	0.58	3.2	381	
Cha I F7	10.30	B5 V	−1.2	—	0.54	3.3	878	
Cha I F8 = HD 95326	8.79	F5 V	3.5	4.3	0.03	—	91	3
Cha I F9 = CPD−76°647	9.58	K0 III	0.7	—	0.62	3.9	196	
Cha I F10	13.74	K3 III	0.3	—	0.77	3.8	1267	
Cha I F11	10.60	B9 V	0.2	0.1	0.86	4.2	233	3
Cha I F12 = HD 95883	7.34	A2 Vn	1.3	1.5	0.00	—	154	3
Cha I F13 = HD 95916	9.23	F8 V	4.0	4.7	0.04	—	89	3
Cha I F15 = HD 96092	7.98	B9 V	0.2	0.7	0.16	—	255	1
Cha I F16	11.47	G2 IV	3.0	—	0.82	3.4	137	
Cha I F18	15.22	G8 III	0.8	—	1.27	4.2	656	
Cha I F20	10.97	K3 V	6.65	—	0.00	—	73	
Cha I F21	11.40	K3 III	0.3	—	0.64	3.3	627	
Cha I F22	14.10	G8 III	0.8	—	1.03	4.1	654	
Cha I F23	12.93	M5 III	−0.3	—	0.88	3.9	911	
Cha I F24 = HD 96675	7.67	B7 V	−0.6	0.2	0.30	3.3	238	1, 4
Cha I F25	13.23	G8 III	0.8	—	1.27	4.3	248	
Cha I F26 = HD 96831	10.13	A1 IV	0.7	—	0.26	3.4	512	
Cha I F28	15.14	K4 III	0.0	—	1.08	5.5	692	
Cha I F30	11.46	K3 III	0.3	—	0.43	4.4	714	
Cha I F31 = HD 97240	8.51	F5 V	3.5	3.4	0.01	—	101	3
Cha I F32	10.53	A7 V	2.2	—	0.52	4.2	170	5
Cha I F33	15.09	G8 III	0.8	—	1.05	4.6	780	
Cha I F35 = HD 97474	8.69	G3 V	4.8	—	0.02	—	58	
Cha I F36	13.76	K0 III	0.7	—	1.22	4.7	292	
Cha I F37 = CPD−75°719	9.56	G9 III	0.75	—	0.32	3.8	330	
Cha I F38 = HD 97901	7.68	A3 IV	1.2	1.2	0.22	—	144	3, 6
Cha I F39 = CPD−76°656	10.07	K3 III	0.3	—	0.30	2.6	628	
Cha I F40 = HD 98143	7.58	B8 III	−1.2	—	0.65	3.3	212	
Cha I F41 = HD 98294	8.52	B8 V	−0.25	—	0.26	3.9	356	
Cha I F42 = HD 98561	8.33	A3.5 IV	1.2	0.6	0.33	3.3	185	3
Cha I F43 = HD 98627	7.38	K5 III	−0.2	—	0.25	3.4	222	
Cha I F44 = HD 98672	6.26	A0 V	0.65	1.2	0.03	—	112	3
Cha I F45 = HD 98913	9.57	F6 V	3.6	3.9	0.01	—	144	3
Cha I F46 = HD 99014	9.72	G2 V	4.7	—	0.05	—	94	
Cha I F47 = HD 99015	6.42	A5 III–IV	1.0	2.2	0.02	—	89	3
Cha I F48 = HD 99161	8.87	B9.5 V	0.4	—	0.18	—	382	
Cha I F49 = HD 99501	9.36	F2 V	3.6	3.9	0.01	—	131	3
Cha I F50 = HD 99515	9.37	A8 IV	2.0	—	0.14	—	244	
Cha I F51 = HD 99591	9.36	F7 V	3.8	4.6	0.05	—	100	3
Cha I F52 = HD 99759	8.48	B9.5 V	0.4	—	0.30	3.3	262	
Cha I F53 = HD 100308	9.37	F6 V	3.6	4.4	0.03	—	114	3
Cha I F54 = HD 100401	8.36	G6 III–IV	2.0	—	0.28	3.4	121	

Notes to Table 1: (see top of next page)

Table 1. (continued)

Notes to Table 1:

1. Photometric absolute magnitude from the study of Corradi et al. (1997).
2. Spectral type from Houk & Cowley (1975). An alternative classification (B2 V; Vrba & Rydgren 1984) gives poorer agreement between spectroscopic and photometric absolute magnitudes.
3. Photometric absolute magnitude and reddening based on data in Table 2.
4. Spectral type from Vrba & Rydgren (1984). An alternative classification (B6 IV/V; Houk & Cowley 1975) gives poorer agreement between spectroscopic and photometric absolute magnitudes.
5. Spectral type from Feigelson & Kriss (1989); reddening from Table 2. An alternative classification (F0 V; Vrba & Rydgren 1984) gives poor agreement in reddening from broadband and Strömgren photometry.
6. Spectral type based on remarks in Houk & Cowley (1975), who classify it as a possible weak Am star.

main sequence (ZAMS) star HD 97300, using the spectrophotometric estimate of its distance (see Sect. 2.2 below), is also shown for comparison with the field stars.

The distribution of points in Fig. 2 allows limits to be placed on the distance of the cloud by visual inspection. Rapid onset of reddening occurs in the range 135–165 pc, indicated by vertical lines in Fig. 2. A distance substantially lower than this range can be excluded as there are several field stars seen in projection against the cloud with distances up to ∼150 pc which have little or no reddening ($E_{B-V} \lesssim 0.05$). This conclusion is consistent with the discussion of Hyland et al. (1982), who note that the lowest distance estimate appearing in the literature (115 pc; Grasdalen et al. 1975) leads to placement of pre-main-sequence stars below the ZAMS in the HR diagram. On the other hand, a distance substantially greater than ∼160 pc can probably also be excluded, as all field stars beyond this have appreciable reddening ($E_{B-V} > 0.1$). Although the distances of individual stars in Fig. 2 may be in error by up to 30% (dependent on spectral type and the method of estimating M_V), a cloud distance >200 pc would require individual distances of as many as 5 field stars with $E_{B-V} > 0.2$ in Fig. 2 to be systematically underestimated by 30% or more, which seems unlikely. Our results therefore argue against the distance of 215 pc favored by Gauvin & Strom (1992), based on the study of Hyland et al. (1982) and Jones et al. (1985), in which it is assumed that the standard 'diffuse cloud' interstellar extinction law (R_V = 3) applies in all lines of sight. Our study of both extinction and interstellar polarization (Whittet et al. 1994) establishes the existence of a non-standard extinction law with R_V up to 5 in the dense central regions of Cha I, in accord with earlier work by Vrba & Rydgren (1984). The value of R_V critically affects the distance estimate for the embedded star HD 97300 (Sect. 2.2); however, only two reddened field stars (F9 and F32) in the critical distance range 120–200 pc have $R_V > 3.5$ (see Table 1).

The reddenings and distances of 213 stars in Kapteyn Selected Area (SA) 203 have been derived from Strömgren *uvby* and Hβ photometry by Franco (1991, 1992). The results provide further evidence relevant to the distance of Cha I and its continuity with reddening material in the region. The centre of SA 203 lies about 2° north of the mid-point of a line joining Cha I and Cha II (compare Fig. 1 of Franco 1991 with our Fig. 1).

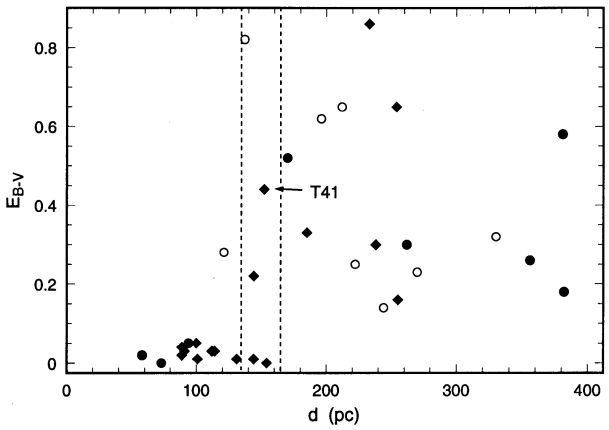

Fig. 2. Plot of reddening E_{B-V} vs. distance d for field stars towards Cha I, using data from Table 1. The locus of the embedded ZAMS star HD 97300 = T41 (Sect. 2.2) is also shown. Diamonds represent stars with absolute magnitudes based on both MK type and *uvby*β photometry; circles represent stars with absolute magnitudes based only on MK type (filled circles: main sequence stars; open circles: giants/subgiants). Vertical lines appear at 135 and 165 pc, which we consider to represent the acceptable range for the distance to the cloud.

The sample does not overlap Cha I but contains stars lying just beyond its eastern boundary. The plot of reddening versus distance for SA 203 displays a sharp front edge at $d \sim 140$ pc (see Fig. 3 of Franco 1991), in reasonable agreement with our result for stars projected in the line of sight of Cha I itself, discussed above (our Fig. 2). Also evident in the SA 203 data set is the occurrence of a well-defined distance (∼ 190 pc) behind which no stars are unreddened. This suggests continuity in the distribution of dust across the region, i.e., a sheet-like structure, lacking 'holes' which would allow more distant stars to be observed with negligible reddening. Comparison of the E_{B-V} vs. d plots for Cha I and SA 203 suggests a high degree of continuity between the cloud and the sheet, although the possibility that the cloud lies behind the sheet at a distance in the range 150–190 pc is not entirely excluded.

We conclude that dust responsible for the onset of reddening in the direction of Cha I is most likely associated with the cloud

Table 2. Strömgren parameters for 14 field stars in the direction of Chamaeleon I, based on observations with the 0.5 m telescope at SAAO in 1997 February.

Star	V	$b-y$	m_1	c_1	β	E_{b-y}
Cha I F8	8.79	0.324	0.145	0.456	2.658	0.021
Cha I F11	10.60	0.593	−0.086	0.839	2.768	0.638
Cha I F12	7.34	0.088	0.170	0.986	2.845	0.000
Cha I F13	9.23	0.360	0.155	0.388	2.628	0.026
Cha I F31	8.53	0.291	0.168	0.417	2.668	0.006
Cha I F32	10.55	0.515	0.045	1.103	2.79:	0.380
Cha I F38	7.70	0.229	0.137	1.042	2.867	0.164
Cha I F42	8.37	0.328	0.078	1.070	2.832	0.237
Cha I F44	6.30	−0.007	0.145	0.898	2.856	0.025
Cha I F45	9.59	0.330	0.158	0.372	2.645	0.010
Cha I F47	6.44	0.116	0.200	0.895	2.840	0.015
Cha I F49	9.31	0.319	0.172	0.402	2.652	0.010
Cha I F51	9.37	0.377	0.166	0.382	2.628	0.039
Cha I F53	9.37	0.352	0.132	0.347	2.624	0.025

itself, and that this onset occurs at

$$d(\text{Cha I}) = 150 \pm 15 \text{ pc}.$$

The result and its uncertainty are estimated by inspection of Fig. 2, allowing for the presence of both reddened and unreddened stars in the distance interval 135–165 pc. It is consistent with our earlier estimate (Whittet et al. 1987) and with that of Steenman & Thé (1989), but inconsistent with the smallest (115 pc) and largest (215 pc) estimates appearing elsewhere in the literature.

2.2. HD 97048 and HD 97300

Cha I contains two late B-type stars, HD 97084 (T32) and HD 97300 (T41), which illuminate prominent reflection nebulae, Ced 111 and Ced 112, respectively. There is general agreement that these stars are embedded members of the young stellar population (e.g. Schwartz 1991) and are thus situated at a distance coincident with that of the cloud itself. HD 97048 is a Herbig Ae/Be star, still approaching the main sequence, and reliable estimation of its distance by spectrophotometric means is difficult because of inherent uncertainty in its luminosity (Assendorp et al. 1990 and references therein). This problem is alleviated for HD 97300 as it has already reached the ZAMS (e.g. Rydgren 1980) and its luminosity is better constrained.

There has been much discussion in the literature on the value of R_V applicable to the line of sight to HD 97300. One approach is to assume the 'standard' diffuse ISM extinction law with R_V = 3.0 (e.g. Hyland et al. 1982); however, it is then impossible to reconcile membership of the T-association with any reasonable geometry for the cloud, as the apparent distances of cloud and star differ by more than 50 pc, and additional problems then arise in understanding the near infrared colours of the star (see Schwartz 1991 for discussion). These objections are removed if a value of $R_V \approx 5$ (e.g. Rydgren 1980; Steenman & Thé 1989; Whittet et al. 1994) is accepted.

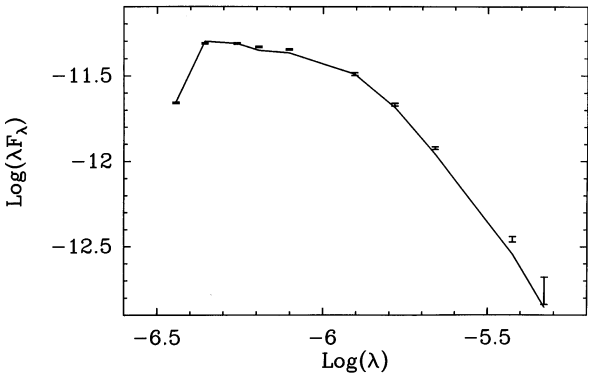

Fig. 3. Spectral energy distribution of HD 97300 (Cha I), calculated from photometric data (points), compared with a model based on reddened intrinsic colours (curve). See text for further details.

The absolute magnitude of HD 97300 is another key issue. The spectral type B9 V seems well established (Houk & Cowley 1975; Rydgren 1980). The absolute magnitude M_V = 0.2 discussed by Steenman & Thé (1989) applies to an 'average' B9 main-sequence star (Schmidt-Kaler 1982), which is inconsistent with the observed Hβ index. However, if one assumes that HD 97300 is on the *zero-age* main sequence, this discrepancy disappears and both spectral type and Hβ index are consistent with an absolute magnitude of M_V = 0.9. The spectral energy distribution of HD 97300 is plotted in Fig. 3 (based on photometry from various references listed in Prusti et al. 1992a). Magnitudes were converted to flux densities using the calibration of Bessell (1979) for *UBVRI* and of Bessell & Brett (1988) for *JHKL*. A model for the spectral energy distribution was constructed using intrinsic colours appropriate to a B9 ZAMS star (Schmidt-Kaler 1982). The best fit (plotted in Fig. 3) occurs for reddening equivalent to a visual extinction of $A_V = 2.23 \pm 0.05$ and an extinction law R_V = 5.0. Taking $M_V = 0.9 \pm 0.2$ and $V = 9.04 \pm 0.01$, we deduce a spectrophotometric distance

$$d(\text{HD 97300}) = 152 \pm 18\text{pc}.$$

This result is in close agreement with our distance estimate for the cloud, based on the reddening distribution of field stars (Sect. 2.1; Fig. 2).

Independent distance estimates based on parallax measurements made by the Hipparcos satellite were recently reported for both HD 97048 and HD 97300 (van den Ancker et al. 1997). Result are listed and compared with those of spectrophotometric methods in Table 3. The parallax distance of HD 97048 has greater precision than that of HD 97300 as the former is about 0.6 mag brighter in V. Note, however, that parallax measurements for both stars are hindered by the presence of circumstellar reflection nebulae. All results in Table 3 are consistent with $d \sim 160$ pc to within the stated errors, although agreement is reached only by assuming that both HD 97048 and HD 97300 lie approximately 1-σ closer than the nominal parallax distance, a somewhat surprising outcome. We suspect that the concordance of the parallax distances for these two stars is probably fortuitous.

Table 3. Summary of results for Chamaeleon I. Parallax data are from van den Ancker et al. (1997).

Sample	Method	Distance (pc)
Cloud extinction	Spectrophotometry (E_{B-V} vs. d)	150 ± 15
HD 97300	Spectrophotometry	152 ± 18
	Parallax	190 ± 40
HD 97048	Parallax	180 ± 20
	Adopted value	160 ± 15

2.3. Summary

The results of the previous sections are summarized in Table 3. Our adopted value of 160 ± 15 pc is consistent with all results to within the errors of measurement. A somewhat smaller distance ($\sim$150 pc) would be favored if the parallax data were disregarded. An appreciably larger distance ($\sim$180 pc) would be favored if greater weighting were given to the parallax data and it were assumed that sheet-like reddening material lies in front of the cloud (Sect. 2.1); however, a distance of 180 pc is somewhat inconsistent with our spectrophotometric distance of HD 97300 (Sect. 2.2) and with our conclusion that Cha I is closer than Cha II (see below).

3. The distance to Chamaeleon II

3.1. HD 111830

Unlike Cha I, Cha II does not contain prominent reflection nebulae, and there is thus no obvious counterpart to HD 97300, the most widely used distance calibrator for Cha I (Sect. 2.2). Inspection of the SERC J films for the Cha II region (fields 21 and 40) reveals the presence of faint, wispy nebulosity, most prominent along the north-eastern boundary of the cloud facing the Galactic plane. This nebulosity does not appear to be illuminated by any individual star or group of stars associated with the cloud, and is most probably a 'limb brightening' effect caused by the interstellar radiation field. Only one star in the region, HD 111830, shows evidence for direct association with optical reflection nebulosity.

HD 111830 (IRAS 12504–7745) is an apparently normal late-type giant of spectral type K0 III (Houk & Cowley 1975), i.e., a 'first-ascent' giant branch star presumed to lack a self-generated dust envelope at the present stage of its evolution (Zuckerman et al. 1995). There is no evidence to suggest that it could be a previously unrecognized pre-main-sequence star: the near infrared colours (Whittet et al. 1991a) are consistent with the optical classification, and the lack of optical variability (comparing data of King 1981, Carrasco & Loyola 1990, Hughes & Hartigan 1992) also argues against interpretation as a T Tauri star. Its association with nebulosity thus appears to be serendipitous. It lies approximately 45 arcmin southwest of the densest region of the Cha II cloud, within a compact, asymmetric reflection nebula approximately 1 arcmin in extent. The entire region surrounding HD 111830 also contains fainter, much more extensive filamentary nebulosity which connects with the main part of Cha II to the north (and also with Cha III to the south), strongly suggesting a continuous structure. We conclude that the dust illuminated by HD 111830 is very probably part of the Cha II complex, and that this star is therefore a useful distance calibrator for the cloud.

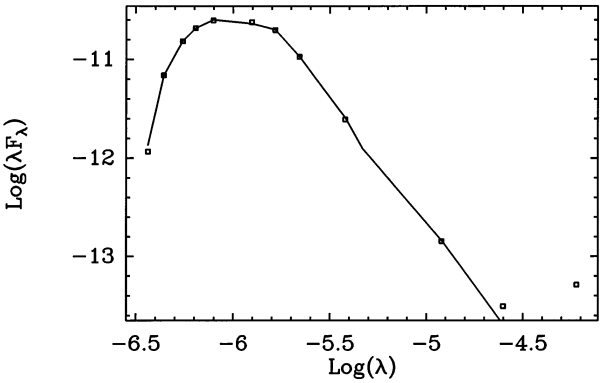

Fig. 4. Spectral energy distribution of HD 111830 (Cha II), calculated from photometric data (points), compared with a model based on reddened intrinsic colours (curve). See text for further details.

The spectral energy distribution of HD 111830 is shown in Fig. 4. This is based on *UBVRI* photometry from Carrasco & Loyola (1990), *JHKL* photometry from Whittet et al. (1991a), and IRAS fluxes from the Serendipitous Survey Catalog (see Whittet et al. 1991a). We have modelled the spectral energy distribution using intrinsic colours for a K0 III star, taken from Bessell (1979), Bessell & Brett (1988) and Waters et al. (1987) for optical, near infrared and $V - [12]$ colors, respectively. At longer wavelengths, the intrinsic curve was assumed to follow a 4500 K blackbody convolved with the IRAS passbands and normalized at 12 μm. Extinction corrections were applied using the R_V-dependent empirical formula of Cardelli et al. (1989). Our best fitting model, illustrated in Fig. 4, is achieved with $R_V = 2.8$ and $A_V = 0.78$, and this gives an excellent fit to the observed broadband fluxes from U (0.35 μm) to the IRAS 12 μm band. Infrared excess emission is apparent at longer wavelengths: this amounts to non-colour-corrected fluxes of 0.1 Jy and 1.0 Jy in the 25 μm and 60 μm IRAS bands, respectively (there is no detection in the 100 μm IRAS band). This emission indicates the presence of warm ($T \sim 80$ K) dust in the vicinity of HD 111830, presumably the same dust that gives rise to the visible reflection nebula.

The absolute visual magnitude of a K0 III star is given as 0.5, 0.7 and 0.8 by Allen (1973), Schmidt-Kaler (1982) and Blaauw (1963), respectively. We adopt $M_V = 0.7 \pm 0.3$, and with $V = 7.78 \pm 0.01$ and $A_V = 0.78 \pm 0.05$, the resulting distance to HD 111830 is

$$d(\text{HD } 111830) = 182 \pm 30 \text{ pc}.$$

The error in d is dominated by the uncertainty in the absolute magnitude.

Table 4. Catalogue of reddenings, distances and related information for field stars in the line of sight to Chamaeleon II, based on broadband *UBVRI* photometry (this paper, Table 6; Hughes & Hartigan 1992). The 'F' notation is from Hughes & Hartigan (1992). Spectral types are from Hughes & Hartigan (1992) unless otherwise indicated in the notes. Absolute magnitudes are deduced from MK spectral types. Infrared photometry from Whittet et al. (1991a) and this paper (Table 7) is used to deduce E_{V-K} and hence $R_V \approx 1.1 E_{V-K}/E_{B-V}$. Intrinsic colours are from Schmidt-Kaler (1982), Bessell & Brett (1988) and Wegner (1994). R_V = 3.1 is assumed when no other value is given. A colon indicates an uncertain value.

Star	V	Sp	$M_V^{\rm sp}$	E_{B-V}	R_V	d (pc)	Notes
Cha II F1	11.72	G5 III	0.9	0.48	—	735	
Cha II F2	10.88	A5 V	1.95	0.56	—	275	
Cha II F3 = CPD−77°877	9.79	F9 V	4.2	0.00	—	131	
Cha II F4 = CPD−77°878	9.63	G2 III	0.9	0.44	2.5:	336	
Cha II F5	11.22	K0 III	0.7	0.24	—	902	
Cha II F6	12.43	B5 V	−1.2	1.13	3.9	699	
Cha II F7	11.07	A7 V	2.2	0.46	—	308	
Cha II F8 = HD 111830	7.78	K0 III	0.7	0.27	2.8	182	1, 2
Cha II F9	15.27	M2 V	9.9	0.00	—	119	
Cha II F10	12.37	F9 V	4.2	0.31	—	277	
Cha II F11	11.40	F0 V	2.7	0.35	—	333	
Cha II F12	12.31	K2 V	6.4	0.01	—	150	
Cha II F13	10.87	G1 V	4.55	0.10	—	159	
Cha II F14	10.30	K3 III	0.3	0.64	—	401	
Cha II F15	9.61	M3 III	−0.6	0.63	—	448	
Cha II F16	13.13	K3 V	6.65	0.01	—	195	
Cha II F17	10.91	K1 III	0.6	0.40	—	652	
Cha II F18	11.03	K3 V	6.65	0.00	—	75	
Cha II F19	11.48	F5 III	1.6	0.30	—	617	
Cha II F20	10.29	K3 III	0.3	0.26	—	687	
Cha II F21 = HD 113074	9.37	B9 V	0.2	0.31	3.1	438	1
Cha II F22	12.36	G1 V	4.55	0.19	—	278	
Cha II F23	9.93	A0 V	0.65	0.40	—	406	
Cha II F24	11.63	M6 III	−0.3	0.44	—	1298	
Cha II F25 = HD 113513	8.86	G5 V	5.1	0.00	—	56	1
Cha II F26	13.32	F4 V	3.5	1.03	—	212	
Cha II F27	12.77	G0 III	1.0	1.32	3.3	304	
Cha II F28 = HD 113693	8.79	K4 V	7.0	0.00	—	23	
Cha II F29	10.25	K1 III	0.6	0.38	—	495	
Cha II F30	9.86	G4 III	0.9	0.13	—	515	
Cha II F31 = CPD−77°888	10.12	B9 V	0.2	0.40	2.8	575	
Cha II F32	12.48	G5 V	5.1	0.11	—	256	
Cha II F33	10.47	F3 V	3.6	0.16	—	188	
Cha II F34 = HD 114503	8.46	B7 V	−0.6	0.19	—	495	
HD 113636	9.96	A0 V	0.65	0.36	3.1	435	1
HD 113758	10.32	A0 V	0.65	0.32	2.9	560	1
HD 113993	9.60	A2 III–IV	0.65	0.30	2.9	413	1
CPD−76°745	10.43	A0 V	0.65	0.30	3.0	597	3
CPD−77°889	10.63	B9.5 V	0.4	0.31	3.0	724	3

Notes to Table 4:

1. Spectral type from Houk & Cowley (1975).
2. See Sect. 3.1 for detailed discussion.
3. Spectral type deduced from *UBV* colours assuming the standard reddening law (E_{U-B}/E_{B-V} = 0.72); results are consistent with one-dimensional classifications given in the SIMBAD data base.

Table 5. Catalogue of reddening, distance and related information for field stars in the SA 203 Quadrant IV region (which contains Chamaeleon II), based on Strömgren *uvbyβ* photometry (Franco 1992; Corradi & Franco 1995; this paper, Table 8). A tick in the final column indicates that the star is seen in projection against the cloud itself (see text). Two stars, CPD−77°877 and HD 113074, are common with Table 4. Absolute magnitudes $M_V^{\rm sp}$ and $M_V^{\rm ph}$ are deduced from the spectral type and Strömgren photometry, respectively; if both are available, d is calculated from the mean. E_{B-V} is calculated from $E_{B-V} = E_{b-y}/0.74$. $R_V \approx 1.1 E_{V-K}/E_{B-V}$ is calculated from infrared photometry in Boulanger et al. (1994), Whittet et al. (1991a) and this paper (Table 7); $R_V = 3.1$ is assumed when no other value is given. A colon indicates an uncertain value.

Star	V	Sp	$M_V^{\rm sp}$	$M_V^{\rm ph}$	E_{B-V}	R_V	d (pc)	Cloud?
SA 203.198 = HD 104036	6.73	A7 V	2.2	2.1	0.02	—	80	
SA 203.205 = HD 104097	9.26	A4 V	1.7	1.8	0.25	—	222	
SA 203.229	10.00	—	—	2.4	0.32	—	210	
SA 203.244	9.68	—	—	3.5	0.04	—	163	
SA 203.269 = HD 105154	9.95	F6 V	3.6	3.8	0.09	—	156	
SA 203.281	10.48	—	—	1.8	0.30	—	355	
SA 203.292	10.12	—	—	0.9	0.24	—	496	
SA 203.294 = HD 105524	9.10	F3 III/IV	2.1	1.4	0.39	2.8	178	
SA 203.305	10.57	—	—	1.2	0.36	—	448	
SA 203.321 = HD 106183	8.58	B8 V	−0.25	0.3	0.34	2.9	326	
SA 203.333 = HD 106247	8.68	F0 IV	2.2	1.4	0.24	—	169	
SA 203.334	10.06	—	—	2.9	0.26	—	187	
SA 203.335	10.59	—	—	2.8	0.25	—	253	
SA 203.341	10.88	—	—	1.3	0.25	—	577	
SA 203.342	10.38	—	—	2.1	0.29	—	296	
SA 203.347	10.55	—	—	3.1	0.34	—	190	
SA 203.352	10.37	—	—	2.7	0.33	—	214	
SA 203.354	9.87	—	—	3.6	0.10	—	156	
SA 203.362	11.13	—	—	2.5	0.28	—	357	
SA 203.365 = HD 106883	9.61	A1 V	1.0	1.1	0.31	3.6	308	
SA 203.366	9.91	—	—	3.2	0.24	—	156	
SA 203.367	10.05	—	—	2.9	0.24	—	191	
SA 203.371	10.87	—	—	2.9	0.27	—	267	
SA 203.373 = HD 107145	6.84	F5 IV/V	3.0	3.2	0.00	—	56	
SA 203.382	10.65	—	—	3.7	0.31	—	158	
SA 203.385	10.21	—	—	1.5	0.27	—	375	
SA 203.389	10.64	—	—	2.0	0.25	—	374	
SA 203.394 = HD 107722	8.27	F6 V	3.6	4.1	0.02	—	74	
SA 203.400	10.53	—	—	3.9	0.25	—	148	
SA 203.402	9.94	—	—	2.9	0.28	—	172	
SA 203.418 = HD 108270	9.38	A4:	—	2.2	0.38	2.9:	164:	√
SA 203.426 = HD 108343	8.02	A8 IV/V	2.2	2.9	0.02	—	121	
SA 203.427 = HD 108378	9.45	F0 III/IV	1.85	1.0	0.37	3.2	233	√
SA 203.443	10.58	—	—	2.8	0.22	—	263	
SA 203.447 = HD 108792	7.52	B9 V	0.2	0.6	0.20	—	200	
SA 203.462 = HD 109067	7.78	F3 IV/V	3.0	3.0	0.00	—	90	
SA 203.496	10.68	—	—	3.9	0.13	—	189	
SA 203.501 = HD 109700	10.29	A9 V:	2.5:	1.0	0.17	—	400:	
SA 203.530 = HD 110336	8.64	B9 IV	−0.2	0.8	0.43	2.8	267	√
SA 203.535	10.66	—	—	2.9	0.17	—	280	
SA 203.537 = HD 110626	8.97	F0 III/IV	1.85	2.1	0.15	—	200	
SA 203.538	10.07	—	—	2.9	0.20	—	204	
SAO 256953 = HD 108927	7.78	B5 V	−1.2	−0.4	0.22	3.0	384	√
SAO 256973 = CPD−76°737	10.25	—	—	3.8	0.04	—	184	√
SAO 256981 = HD 111152	8.45	F5 V	3.5	3.2	0.01	—	103	
SAO 256984 = CPD−77°877	9.78	F9 V	4.2	3.9	0.03	—	134	√
SAO 257004 = HD 113074	9.40	B9 V	0.2	0.4	0.30	3.1	431	√
SAO 257007 = HD 113263	8.67	F2 IV	2.4	3.0	0.04	—	148	√

3.2. The distribution of reddening

Tables 4 and 5 list field stars for which distance and reddening information are available in the direction of Cha II and its environs. These tables are based on distinct data sets in which optical broadband (*UBVRI*) and Strömgren (*uvbyβ*) photometry is used to determine stellar parameters (Hughes & Hartigan 1992; Franco 1991, 1992). They also sample distinct areas of sky. The Hughes & Hartigan stars occupy an area approximately $1.5^\circ \times 1.5^\circ$, centered at Galactic coordinates $\ell \approx 303.5^\circ$, $b \approx -15^\circ$, coincident with the part of the cloud occupied by the embedded T-association. The Franco stars occupy a larger area of sky bound by coordinates $300 < \ell < 305^\circ$, $-16 < b < -12^\circ$ (Quadrant IV of the SA 203 field); those stars lying towards the dark cloud itself (bound approximately by coordinates $301.5 < \ell < 304.5^\circ$, $-15.5 < b < -13.0^\circ$; see Fig. 2 of Corradi et al. 1997) are identified by a 'tick' in the right-hand column of Table 5.

We have extended our database by complementing broadband photometry available in the literature with additional observations made with telescopes at SAAO, presented in Tables 6 and 7. *UBVRI* photometry (Table 6) was obtained in 1995 April and July with the Modular Photometer on the 0.5-m telescope, and *JHKL* photometry (Table 7) was obtained in 1995 April and 1996 January with the Mk III Infrared Photometer on the 1.9-m telescope. In both cases, results were reduced to the standard SAAO photometric systems.

Absolute magnitudes for all stars in Table 4 are deduced from spectral types using the calibration of Schmidt-Kaler (1982). Intrinsic $B-V$ colours from Schmidt-Kaler (1982) are used to determine E_{B-V}. The approximation $R_V \approx 1.1 E_{V-K}/E_{B-V}$ is used to calculate the ratio of total to selective extinction, with K-band photometry from Whittet et al. (1991a) and this paper (Table 7). Intrinsic $V-K$ colours are from Bessell & Brett (1988) for spectral types B8–K4, and from Wegner (1994) for spectral types B5–B7.

In addition to field stars in quadrant IV of SA 203 observed by Franco (1992), Table 5 contains previously unpublished data for six field stars observed in 1992 April with the Strömgren Automatic Telescope at the European Southern Observatory (ESO), the same instrument used in the Franco (1992) study. Strömgren parameters for these stars are listed in Table 8. Reddening values for all stars in Table 5 are presented in the Johnson system (converted from the Strömgren system). Absolute magnitudes are deduced from *uvbyβ* photometry (Franco 1991) or from MK spectral types, where available (Schmidt-Kaler 1982). The agreement between photometric and spectroscopic absolute magnitudes is generally good; an average value was adopted for the distance determination.

Information on the interstellar extinction law in Cha II is limited by the availability of infrared photometry, which is much less extensive than for Cha I. Estimates of R_V are listed in Tables 4 and 5 for a total of 19 stars. The average value, ∼3.0, is close to that for the diffuse interstellar medium, and in only a very few cases is there evidence for significantly larger values. This apparent difference compared with results for Cha I (Table 1) may be a selection effect, with fewer dense regions being sampled in Cha II. For all stars in which R_V is undetermined in Tables 4 and 5, distances are calculated assuming conversion of reddening to total extinction via the standard average, i.e. $A_V = 3.1 E_{B-V} = 4.2 E_{b-y}$.

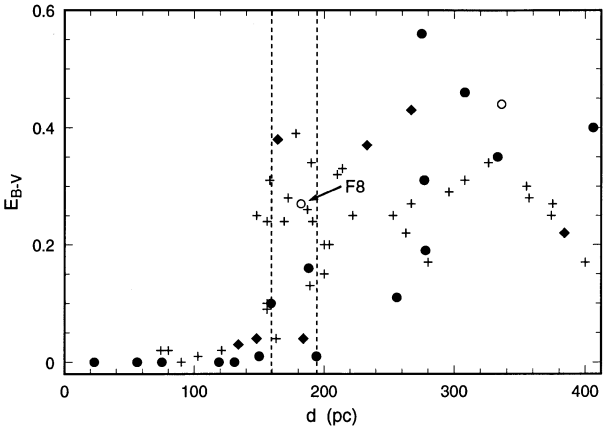

Fig. 5. Plot of reddening E_{B-V} vs. distance d for field stars in the Cha II region. Data from Table 4 (broadband photometry) are plotted as filled circles (main sequence stars) and open circles (giants/subgiants). Data from Table 5 (Strömgren photometry) are plotted as diamonds for stars seen in projection against the cloud itself (identified in the right hand column of Table 5) and as crosses for the remainder. The star labelled F8 is HD 111830 (see Sect. 3.1). Vertical lines appear at 160 and 195 pc, which we consider to represent the acceptable range for the distance to the cloud.

Fig. 5 plots E_{B-V} against distance for stars in Tables 4 and 5. Plotting symbols have the same meaning as in Fig. 2, with the additional distinction of stars from Table 5 located on and off (adjacent to) the cloud. Vertical lines indicate distances of 160 and 195 pc. We treat these values as approximate upper and lower limits for the distance of Cha II: below ∼160 pc, there is a dearth of stars with significant reddening (i.e., with $E_{B-V} > 0.05$), and above ∼195 pc, there are none that *lack* significant reddening.

The absence of distant unreddened stars supports the presence of sheet-like material towards Cha II. As in the case of Cha I, the question then arises: is the cloud embedded in the sheet, or are they unconnected? We note that stars located on and off the cloud have similar reddening-distance distributions, both in our dataset (Fig. 5) and in the more extensive study of Corradi et al. (1997) of the entire Chamaeleon-Musca-Crux region (see Sect. 5), consistent with physical association. The morphology of Cha II and its environs provides further guidance: if the cloud lay behind the sheet, or close to its rear edge, the filamentary reflection nebulosity which pervades the region (Sect. 3.1) should appear as striations across the face of the dark cloud, which is not in fact the case. The possibility that Cha II lies in front of the sheet is more difficult to exclude on morphological grounds, but we note that the filamentary nebulosity shows some positional correlation with the edges of the cloud. We conclude that cloud and sheet are, in all probability, physically associated.

Table 6. Mean *UBVRI* photometry for 10 field stars in the direction of Chamaeleon II, obtained with the 0.5-m telescope at SAAO in 1995 April and July. The number of observations in the mean (n) is given in the right hand column. Standard deviations are $\leq$0.01 mag in all passbands.

Star HD/CPD	V	$B-V$	$U-B$	$V-R$	$V-I$	n
113074	9.372	0.236	−0.080	0.154	0.350	2
113636	9.959	0.334	0.176	0.193	0.439	4
113758	10.315	0.293	0.181	0.163	0.377	3
113993	9.601	0.346	0.214	0.190	0.418	3
114503	8.461	0.058	−0.248	0.038	0.103	2
–76°742	10.781	0.680	0.169	0.376	0.753	2
–76°745	10.430	0.278	0.199	0.145	0.338	2
–77°878	9.631	1.206	0.936	0.646	1.275	3
–77°888	10.123	0.327	0.175	0.188	0.414	3
–77°889	10.630	0.256	0.092	0.143	0.340	3

Table 7. *JHKL* photometry for 9 field stars in the direction of Chamaeleon II, obtained with the 1.9-m telescope at SAAO in 1995 April ('F' stars) and 1996 January (SA stars). Errors are <0.02 mag in all passbands.

Star	$J-H$	$H-K$	K	$K-L$
Cha II F4	0.61	0.12	6.77	0.16
Cha II F6	0.53	0.25	8.82	—
Cha II F27	1.03	0.31	7.12	0.17
Cha II F31	0.10	0.05	9.28	—
SA 203.294	0.34	0.08	7.21	—
SA 203.321	0.06	0.01	8.04	—
SA 203.365	0.16	0.05	8.52	—
SA 203.418	0.22	0.06	8.06	—
SA 203.427	0.30	0.09	7.68	—

3.3. Summary

We conclude from Fig. 5 and the above discussion that the best estimate for the distance to Cha II is

$$d(\text{Cha II}) = 178 \pm 18 \text{ pc}.$$

This value assumes a location for the cloud near the mid-point of the distance interval 160–195 pc in which both reddened and unreddened stars are found, and the probable error reflects this distribution. Our result is consistent with the calculated distance to the embedded star HD 111830 (Sect. 3.1), and marginally inconsistent with the distance of 200 pc to the cloud favored by Hughes & Hartigan (1992).

Comparing results for Cha I and Cha II, it seems probable that Cha II is somewhat more distant, although distances ∼160–170 pc for both clouds would be within the uncertainties.

4. Infrared fluxes of T Tauri stars

Schwartz (1991) noted that T Tauri stars in Cha II appear to be around 1–2 magnitudes fainter in visual apparent magnitude than their counterparts in Cha I, suggestive of a greater distance for Cha II if intrinsic luminosities are similar. However, this difference seems to be due at least in part to greater average extinction for the Cha II population (Hughes & Hartigan 1992). A more reliable comparison is provided by flux measurements in the IRAS passbands, as interstellar extinction may be neglected at these wavelengths. Gregorio Hetem et al. (1988) and Hughes et al. (1989) noted independently that average IRAS fluxes of T Tauri stars in Cha II are lower than in Cha I. These authors estimate the distance to Cha II on the basis of this difference and an assumed distance to Cha I, but with inconsistent results (Gregorio Hetem et al. and Hughes et al. estimate Cha II to be 16% and 40% more distant than Cha I, respectively). No details of which stars were included in these estimates, or how they were selected, are given in either case.

Table 8. Strömgren parameters for 6 field stars in the direction of Chamaeleon II, based on observations with the ESA Strömgren Automatic Telescope in 1992 April.

Star	V	$b-y$	m_1	c_1	β	E_{b-y}
SAO 256953	7.778	0.098	0.069	0.502	2.720	0.162
SAO 256973	10.245	0.385	0.148	0.375	2.607	0.031
SAO 256981	8.451	0.291	0.158	0.478	2.670	0.011
SAO 256984	9.784	0.365	0.178	0.379	2.627	0.021
SAO 257004	9.404	0.184	0.067	0.763	2.781	0.225
SAO 257007	8.666	0.279	0.142	0.553	2.693	0.031

Table 9 lists IRAS 12, 25 and 60 μm fluxes for low-mass pre-main-sequence (PMS) stars in the two clouds, taken from the results of Whittet et al. (1991a, b). To delimit the sample, we adopted the following criteria:

(i) To be selected, an object must be an unconfused IRAS source detected at 12, 25 and 60 μm, lying in the "T Tauri box" in the [25]–[12], [60]–[25] colour-colour diagram (Harris et al. 1988; see Fig. 2 of Whittet et al. 1991a and Fig. 3 of Whittet et al. 1991b).

(ii) The optical counterpart must be a pre-main-sequence candidate identified in the Hα survey of Schwartz (1977).

(iii) Additionally, three objects in Cha I satisfying the above criteria but considered too luminous to be low-mass T Tauri stars (Sz19; Sz25 = HD 97048; Sz42; see Prusti et al. 1992a) were omitted.

On this basis we select 10 objects in Cha I and 9 in Cha II. The results in Table 9 show that T Tauri stars in Cha I are on average a factor ~ 1.6 brighter in each of the IRAS bands. If the mean luminosities are assumed to be the same, the distance ratio is

$$\frac{d(\text{Cha II})}{d(\text{Cha I})} = \left[\frac{F(\text{Cha I})}{F(\text{Cha II})}\right]^{\frac{1}{2}} \approx 1.26$$

where F is mean flux. This may be compared with the ratio of our results in the previous sections: $d(\text{Cha II})/d(\text{Cha I}) \sim 1.1$. Thus, the T Tauri fluxes give some support to the conclusion that Cha II is significantly more distant than Cha I.

Table 9. IRAS fluxes at 12, 25 and 60 μm (in Jy without colour correction) for T Tauri stars in Cha I and Cha II, selected using criteria described in the text. 'Sz' numbers are from Schwartz (1977). IRAS data are from Whittet et al. (1991a, b).

Star	IRAS	[12]	[25]	[60]
Sz2	10548–7708	0.55	0.82	0.81
Sz3	10552–7655	0.24	0.52	0.66
Sz4	10564–7643	0.08	0.19	0.24
Sz5	10577–7706	0.21	0.37	0.60
Sz6	10578–7645	1.12	1.70	1.50
Sz11	11027–7611	0.70	0.96	0.84
Sz17	11057–7616	0.10	0.15	0.24
Sz29	11074–7645	0.12	0.22	0.26
Sz37	11093–7701	0.42	0.88	1.08
Sz39	11101–7603	0.38	0.53	0.69
	Mean Chamaeleon I:	0.39	0.63	0.69
Sz49	12571–7637	0.09	0.14	0.20
Sz50	12571–7654	0.22	0.53	0.89
Sz51	12581–7735	0.13	0.20	0.24
Sz53	13011–7714	0.09	0.15	0.20
Sz54	13014–7723	0.42	0.48	0.31
Sz58	13030–7707	0.37	0.48	0.94
Sz59	13031–7714	0.31	0.36	0.40
Sz60	13035–7721	0.11	0.12	0.11
Sz61	13040–7738	0.48	0.70	0.70
	Mean Chamaeleon II:	0.25	0.35	0.44
	Mean Cha I/Cha II:	1.6	1.8	1.6

5. Sheet geometry

King et al. (1979) and King (1981) propose that the entire South Celestial Pole region contains a layer of interstellar material, underlying the Galactic plane and roughly parallel to it at an altitude of 40–80 pc. This conclusion is reached by considering the vertical distances from the Galactic plane of a number of stars illuminating reflection nebulae (including HD 97300 in Cha I and HD 111830 in Cha II). If the Chamaeleon clouds are, indeed, embedded in a structure of this nature, their distances are given by the equation

$$d = z_{\rm s} \csc |b|$$

where $z_{\rm s}$ is the vertical distance of the sheet below the Galactic plane, and b is Galactic latitude. This equation gives values consistent with our results from Sects. 2 and 3 if $z_{\rm s} \approx 40$–45 pc, i.e. close to the low end of the range suggested by King et al. (1979). The predicted ratio of distances is d(Cha II)/d(Cha I) $\sim$ 1.14, independent of $z_{\rm s}$, consistent the conclusion that Cha II is more distant than Cha I.

The parallel sheet model of King et al. is in contrast to the results of Corradi et al. (1997) for regions closer to the Galactic plane. From an extensive study of reddening vs. distance for 1017 stars in Chamaeleon-Musca-Crux (Corradi & Franco 1995), these authors argue that continuous sheet structure extends from the Chamaeleon region at $b \approx 15^\circ$ towards the Coalsack at $b \approx 0^\circ$. The distribution of reddening towards the Coalsack, Chamaeleon and intermediate clouds in Musca implies comparable distances (150 $\pm$ 30 pc) for dust in all of these regions, suggestive of sheet structure roughly perpendicular (rather than parallel) to the Galactic plane. However, it is possible that a warped sheet, or intersecting sheets, might accommodate both scenarios. There is some hint in Fig. 1a that we may be observing two intersecting layers of material in the Chamaeleon region (e.g. roughly perpendicular striations meet at Cha III). It would be of interest to investigate the distances of clouds at higher latitude, mapped by Keto & Myers (1986), as these may lie within the extension of sheet structure away from the Galactic plane.

6. Chamaeleon III and DC 300.2–16.9

No data are available to allow detailed plots of colour excess vs. distance for Cha III and DC 300.2–16.9. Only three stars in the photometric study of Corradi & Franco (1995) lie in the general direction of Cha III (SAO 256924, 256930 and 256999; see figure 2 of Corradi et al. 1997), but these are all foreground objects with low reddening and distances in the range 86–106 pc. Thus, we can merely conclude that $\sim$106 pc is a reasonable lower limit on the distance to Cha III. Only one star (SAO 256886) in the Corradi & Franco study lies toward DC 300.2–16.9; interestingly, this object is appreciably reddened ($E_{B-V} \approx 0.24$) and at a distance $\sim$150 pc, which can be taken as an approximate upper limit on the probable distance to this cloud. Three reddened stars (HD 102065, 103536 and 103875) from the study of Boulanger et al. (1994) lie close to the southern boundary of DC 300.2–16.9; as their estimated distances (170–470 pc; see Table 2 of Boulanger et al.) are greater than that of SAO 256886, they probably lie behind the cloud.

These limits are consistent with geometrical scenarios discussed in Sect. 5 and the probable association of both clouds with sheet-like structure. The csc $|b|$ (parallel sheet) model predicts $d \sim 140$ pc for Cha III and $d \sim 150$ pc for DC 300.2–16.9, whereas the perpendicular sheet model proposes $d \sim 150$ pc for all clouds associated with the sheet. Thus, distances in the range 140–160 pc for both Cha III and DC 300.2–16.9 seem consistent with all currently available constraints.

7. Conclusions and future work

From an examination of the distribution of reddening, we deduce distances of 160 $\pm$ 15 pc and 178 $\pm$ 18 pc to the Cha I and Cha II dark clouds, respectively. Although the clouds could share a common distance to within observational error, we present independent evidence to suggest that Cha II is the more distant by $\sim$10–25%. Both appear to be part of a macroscopic sheet structure that extends over much of the Chamaeleon-Musca-Crux region. If Cha III and DC 300.2–16.9 are physically connected with Cha I and Cha II, as suggested by the distribution of 100 μm flux, then their distances are comparable and likely in the range 140–160 pc, dependent on the assumed geometry. It seems unlikely that these results can be further improved by spectrophotometric techniques.

Parallax measurements from Hipparcos are available to date for only two stars in Cha I, and none in Cha II. Further data are anticipated: the CD-ROM version of the Hipparcos Input Catalogue (Turon et al. 1992) contains about a third of our Cha I stars, and a rather smaller fraction – including HD 111830 – in Cha II. (Hipparcos is complete down to about $V = 7.5$; almost all stars down to $V = 9$ and a few fainter ones are included). A median accuracy of about one milliarcsec is expected for stars with $V < 9$; thus, a star at $d \sim 150$ pc will have a typical error in parallax of $\sim$15%, corresponding to an error in distance of about $\pm$20 pc (as for HD 97048), comparable with the smallest errors in individual stellar distances determined spectrophotometrically. However, the parallax distance error increases rapidly for fainter and more distant stars. It is therefore unlikely that Hipparcos data for field stars will dramatically improve the reddening-distance plots in Figs. 2 and 5, although some refinement can be expected, e.g. in the case of the embedded K giant HD 111830, currently limited by a rather imprecise absolute magnitude.

Acknowledgements. We are grateful to the Director, SAAO, for observing time, and to Greg Roberts and Francois van Wyk (SAAO) for obtaining *UBVRI* photometry of selected stars in Cha II. We also thank Mario van den Ancker and his collaborators for allowing us access to their Hipparcos results prior to publication. This research has made use of the SIMBAD database, operated at CDS, Strasbourg, France, and was partly funded by National Science Foundation grant AST–9419690. G.A.P.F. thanks the Brazilian Agency CNPq for partial support. K.A.L. thanks the Astronomical Society of New York for travel funding. Finally, we thank an anonymous referee for detailed comments which led to significant improvements to this paper.

References

Alcalá J.M., Covino E., Franchini M., Krautter J., Terranegra L., Wichman R., 1993, A&A 272, 225
Allen C.W., 1973, *Astrophysical Quantities*, University of London, Athlone Press
Assendorp, R., Wesselius, P.R., Whittet, D.C.B., Prusti, T., 1990, MNRAS 247, 624
Bessell M.S., 1979, PASP 91, 589
Bessell M.S., Brett, J.M., 1988, PASP 100, 1134
Blaauw A., 1963, in *Basic astronomical data*, ed. K.A. Strand, University of Chicago Press, p. 383
Boulanger F., Prévot M.L., Gry, C., 1994, A&A 284, 956
Cardelli J.A., Clayton G.C., Mathis J.S., 1989, ApJ 345, 245
Carrasco G., Loyola P., 1990, A&AS 82, 553
Chen H., Grenfell T.G., Myers, P.C., Hughes, J.D., 1997, ApJ 478, 295
Corradi W.J.B., Franco G.A.P., 1995, A&AS 112, 95
Corradi W.J.B., Franco G.A.P., Knude J., 1997, A&A in press
Crawford D.L., 1975a, PASP 87, 481
Crawford D.L., 1975b, AJ 80, 955
Crawford D.L., 1978, AJ 83, 48
Crawford D.L., 1979, AJ 84, 1858
Feigelson, E.D., Kriss, G.A., 1989, ApJ, 338, 262
FitzGerald M.P., 1974, A&A 32, 465
FitzGerald M.P., Stephens T.C., Witt A.N., 1976, ApJ 208, 709
Franco G.A.P., 1991, A&A 251, 581
Franco G.A.P., 1992, A&AS 93, 373
Gauvin L.S., Strom K.M., 1992, ApJ 385, 217
Graham J.A., Hartigan P., 1988, AJ 95, 1197
Grasdalen G., Joyce R., Knacke R.F., Strom S.E., Strom K.M., 1975, AJ 80, 117
Gregorio Hetem J.C., Sanzovo G.C., Lépine J.R.D., 1988, A&AS 76, 347
Harris S., Clegg P., Hughes J., 1988, MNRAS 235, 441
Hartigan P., 1993, AJ 105, 1511
Houk N., Cowley A.P., 1975, *University of Michigan catalogue of two-dimensional spectral types for the HD stars*, vol. 1
Hughes J.D., Emerson J.P., Zinnecker H., Whitelock P.A., 1989, MNRAS 236, 117
Hughes J.D., Hartigan P., 1992, AJ 104, 680
Hughes J.D., Hartigan P., Graham J.A., Emerson J.P., Marang F., 1991, AJ 101, 1013
Hyland A.R., Jones T.J., Mitchell R.M., 1982, MNRAS 201, 1095
Jones T.J., Hyland A.R., Harvey P.M., Wilking B.A., Joy M., 1985, AJ 90, 1191
Keto E.R., Myers P.C., 1986, ApJ 304, 466
King D.J., 1981, Ph.D. Thesis, University of New South Wales
King D.J., Taylor K.N.R., Tritton K.P., 1979, MNRAS 188, 719
Knee L.B.G., 1992, A&A 259, 283
Knee L.B.G., Prusti T., 1996, A&A 312, 455
Larson K.A., Prusti T., Whittet D.C.B., 1997, A&A in preparation
Laureijs R.J., Chlewicki G., Clark F.O., Wesselius P.R., 1989, A&A 220, 226
Nisini B., Lorenzetti D., Cohen M., et al., 1996, A&A 315, L321
Prusti T., Whittet D.C.B., Wesselius P.R., 1992a, MNRAS 254, 361
Prusti T., Whittet D.C.B., Assendorp R., Wesselius P.R., 1992b, A&A 260, 151
Rydgren A.E., 1980, AJ, 85, 444
Schmidt-Kaler Th., 1982, in: *Landolt-Börnstein New Series*, Group IV, Volume 2b, eds. K. Schaifers & H. H. Voigt, p. 1
Schwartz R.D., 1977, ApJS 35, 161
Schwartz R.D., 1991, in *Low mass star formation in southern molecular clouds*, ed. B. Reipurth, ESO Scientific Report no. 11, p. 93
Steenman H., Thé P.S., 1989, ApSS 161, 99
Turon C., et al., 1992, European Space Agency SP–1136
van den Ancker M.E., Thé P.S., Tjin A Djie H.R.E., Catala C., de Winter D., Blondel P.F.C., Waters L.B.F.M., 1997, A&A 324, L33
Vrba F.J., Rydgren A.E., 1984, ApJ 283, 123
Waters L.B.F.M., Coté J., Aumann H.H., 1987, A&A 172, 225
Wegner W., 1994, MNRAS 270, 229
Whittet D.C.B., Kirrane T.M., Kilkenny D., Oates A.P., Watson F.G., King D.J., 1987, MNRAS 224, 497
Whittet D.C.B., Assendorp R., Prusti T., Roth M., Wesselius P.R., 1991a, A&A 251, 524
Whittet D.C.B., Prusti T., Wesselius P.R., 1991b, MNRAS 249, 319
Whittet D.C.B., Gerakines P.A., Carkner A.L., Hough J.H., Martin P.G., Prusti T., Kilkenny D., 1994, MNRAS 268, 1
Zuckerman B., Kim S.S., Liu T., 1995, ApJ, 446, L79

This article was processed by the author using Springer-Verlag LaTeX A&A style file *L-AA* version 3.